Cyclic nigerosyl-1,6-nigerose-based nanosponges: An innovative pH and time-controlled nanocarrier for improving cancer treatment

Cyclic nigerosyl-1,6-nigerose-based nanosponges: an innovative pH and time-controlled nanocarrier for improving cancer treatment

F. Caldera[1*], M. Argenziano[2*], F. Trotta[1], C. Dianzani[2], L. Gigliotti[3], M. Tannous[1], L. Pastero[4], D. Aquilano[4], T. Nishimoto[5], T. Higashiyama[6], R. Cavalli[2]

[1]Dipartimento di Chimica – Università di Torino. Via P. Giuria 7, 10125 Torino – Italy
[2]Dipartimento di Scienza e Tecnologia del Farmaco – Università di Torino. Via P. Giuria 9, 10125 Torino – Italy
[3] Dipartimento di Scienze della Salute, UPO, via Solaroli 17, 28100 Novara - Italy
[4]Dipartimento di Scienze della Terra, Università di Torino. Via V. Caluso 35, 10125 Torino – Italy
[5]Division Manager New Material Development Division R&D Center Hayashibara Co., Ltd. 675-1 Fujisaki, Naka-ku, Okayama 702-8006, Japan
[6]NAGASE (EUROPA) GmbH/ Hayashibara - Immermannstrasse 65c, 40210 Düsseldorf, Germany

***** Equal contribution to the work.

Corresponding author:
Roberta Cavalli,
Department of Drug Science and Technology,
University of Turin
Via Pietro Giuria 9,
10125 Turin, Italy
Phone: +390116707190
Fax: +390116707687
e-mail: roberta.cavalli@unito.it

Abstract

The design and structural optimisation of a novel polysaccharide-based nanomaterial for the controlled and sustained release of doxorubicin are here reported. A cross-linked polymer was obtained by reacting a tetraglucose, named cyclic nigerosyl-1-6-nigerose (CNN), with pyromellitic dianhydride. The cross-linking reaction formed solid nanoparticles, named nanosponges, able to swell as a function of the pH. Nanoparticle sizes were reduced using High Pressure Homogenization, to obtain uniform nanosuspensions. Doxorubicin was incorporated into the CNN-nanosponges in a good extent. DSC and solid state NMR analyses proved the drug interaction with the polymer matrix. *In vitro* studies demonstrated pH-dependent slow and prolonged release kinetics of the drug from the nanoformulation. Doxorubicin-loaded CNN-nanosponges were easily internalized in A2780 cell line. They might considered an intracellular doxorubicin reservoir, able to slowly release the drug over time. CNN-nanosponges may be promising biocompatible nanocarriers for the sustained delivery of doxorubicin with potential localised application in cancer treatments.

Keywords: CNN, nigerose, nanosponges, doxorubicin, sustained release

1. Introduction

Controlled and sustained release delivery systems of drugs may open up new avenues in nanotherapeutic fields to overcome some drug limitations, with spatial and time-controlled release kinetics (Arpicco et al., 2016, Prasad at al., 2018). A number of these formulations have used nanoscaled carriers encapsulation. Indeed, drug delivery system-based nanoparticles, able to store and release molecules for an extended period of time (weeks or months) and as a function of an external stimulus, can play a key role in developing safer and more effective nanomedicines (Mura, Nicolas & Couvreur, 2013). The use of nanocarriers allows for the modulation and modification of the physico-chemical properties of drugs, producing improved pharmacokinetics and bio-distribution profiles (Hamidi, Azadi, Rafiei & Ashrafi, 2013). Various biodegradable and biocompatible polymer systems could be used as interesting advanced controlled-release systems for bioactive molecules (Duchene, Cavalli & Gref, 2016). Polymer nanoparticles are easy to produce with improved stability and more control over drug release (Jaimes-Aguirre, et al., 2016). Indeed, drug release kinetics can be precisely controlled by the physico-chemical properties of the polymer, such as molecular weight, porosity, hydrophobicity and crystallinity (Bhattacharjee et al., 2016). Moreover, the presence of specific moiety in the polymer structure, responsive to external stimuli, i.e. dissociable carboxylic groups or redox reactive groups, may facilitate localised drug delivery (Liu, Yang & Urban, 2017).

Notably, prolonged-release polymer nanoparticles can reduce the frequency of administration of drugs, particularly those with a short half-life, stabilise drug absorption, decrease the occurrence of adverse side effects and improve patients' adherence to therapy (Natarajan, Nugraha, Ng & Venkatraman, 2014). In particular, poly(lactic-co-glycolic acid (PLGA), a biodegradable polyester approved for human use, has been extensively studied to obtain sustained release nanovectors. Much attention in research has been focused on designing PLGA nanosystems for the controlled delivery of anticancer drugs (Dinarvand, Sepehri, Manoochehri, Rouhani & Atyabi, 2011, Khan et al., 2016). A number of PLGA nanoparticles were studied for doxorubicin, tuning the formulation design to obtain prolonged release kinetics. Doxorubicin-loaded PLGA nanoparticles with the surface modified with poly(L-γ-glutamic acid) (γ-PGA) and finally conjugated with folic acid showed a release profile lasting over 7 days (Jaimes-Aguirre et al., 2017).

Cross-linked polymer nanoparticles represent an alternative formulation approach. Recently, cyclodextrin-based nanosponges, hyper cross-linked cyclodextrin polymers, with sizes in the nanometer order of magnitude, have been designed as a drug delivery nanosystem (Trotta, Zanetti & Cavalli, 2012, Liang et al.,2013, Trotta, Dianzani, Caldera, Mognetti & Cavalli, 2014, Caldera,

Tannous, Cavalli, Zanetti & Trotta, 2017, Liang et al., 2017, Sherje, Dravyakar, Kadam, Jadhav, 2017). Cyclodextrins are a class of cyclic glucopyranose oligomers with a characteristic toroidal shape that forms a well-defined truncated cone-shaped lipophilic cavity. Cyclodextrins are able to include compounds whose geometry and polarity are compatible with that of their cavity (Muankaew & Loftsson, 2018). Cyclodextrin-based nanosponges exhibited a superior inclusion capability than parent cyclodextrins. Indeed, they were able to incorporate many types of molecules, such as small molecules, macromolecules and gases (Trotta et al., 2014, Swaminathan et al., 2010a, Cavalli et al., 2010). The loaded molecules are generally delivered with a slow and prolonged release profile, according to the nanoparticle network structure. Indeed, the release can be influenced by the cross-linking ratio and the nature of the polymer mesh to obtain a sustained and controlled delivery (Swaminathan et al., 2010b, Torne, Ansari, Vavia, Trotta & Cavalli, 2010, Daga et al., 2016, Gigliotti et al., 2017). The incorporation and storage capability is strongly affected by the polymer nanostructure, as well as the presence of many cyclodextrin cavities able to cooperate. To load hydrophilic or charged molecules, modifications of nanosponges were devised. Interestingly, the introduction of charged groups either in the nanostructure or on the surface of nanosponges enabled the production of further interaction sites for loading dissociable drugs (Lembo et al., 2013, Bastiancich et al., 2014). Based on these premises and to expand the possibility of controlling the release, another cyclic oligosaccharide. i.e. a tetraglucose, was selected as a building block of new nanosponges, in place of cyclodextrins (Wei, et al. 2015). Intriguingly, cyclic nigerosyl-1-6-nigerose**, (**CNN**)** is a non-reducing cyclic tetrasaccharide with a unique structure consisting of four D-glucopyranosyl molecules connected by alternate α-(1-3) and α-(1-6) glycosidic bonds (Fig. 1A)**.** CNN differs from cyclodextrin not only due to its number of glucose units (4) and type of glucosidic bond, but also due to the arrangement of the hydroxyl groups. Namely, two of them are oriented toward the inner cavity of CNN, making it quite polar.

This cyclic tetrasaccharide is obtained from hydrolysed starch by the action of a mixture of enzymes (Nishimoto et al., 2002, Aga et al., 2003). Cyclotetraglucose occurs naturally in sake lees (i.e., the sediment that forms during rice wine production), in sake itself and in food-grade starch (e.g., tapioca starch, cornstarch) (Watanabe et al., 2004). The industrial manufacturing production is done by Hayashibara (Japan). This tetraglucose is a white crystalline powder which is safe and stable to temperature, while at alkaline pH values a slow degradation was observed (Weissenfeld, 2005). The capacity to interact as such with various molecules was studied. The complexation of some aromatic compounds with CNN was investigated, showing the formation of guest-CN complexes with vanillin, cinnamaldehyde and eugenol (Ishikawa, Kuwano, Chaen & Matsumoto,

2009). Moreover, CNN have been used for powdering tocopherol, vitamin D and EPA (Oku et al., 2007).

This work aims at exploiting the CNN unit as a monomer for the synthesis of new cross-linked polymers, called CNN-nanosponges (CNN-NS). To obtain the CNN-based polymer, a synthetic protocol was tuned, selecting pyromellitic dianhydride (PMDA) as a cross-linker (Figure 1B).

Firstly, three types of CNN-NS will be considered varying the molar ratio between CNN and pyromellitic dianhydride (i.e. 1:2, 1:4, 1:6 ratios, respectively) to optimise the nanostructure for drug delivery. Their physico-chemical characterisation will be studied and the drug loading capability will be investigated using doxorubicin as the model molecule. Finally, the *in vitro* biological behaviour of doxorubicin-loaded CNN-NS will be evaluated.

2. Material and methods

2.1 Materials

Cyclic nigerosyl-1-6-nigerose (CNN) was received as a kind gift from Hayashibara (Japan). Doxorubicin hydrochloride and pyromellitic dianhydride (PMDA) were purchased from Sigma. Solvents and reagents, unless otherwise indicated, were analytical-grade commercial products, used as received.

2.2 CNN-nanosponges synthesis

The quantities of chemicals used for the synthesis of the three NS are listed in table 1. In summary, 4.886 g of CNN, desiccated in an oven at 100°C up to constant weight, were solubilised in 20 mL of dimethyl sulfoxide (DMSO) at room temperature. Subsequently, 5 mL of triethylamine (Et_3N) and, after a few minutes, the correct amount of pyromellitic dianhydride were added. The solution was vigorously stirred until gelation point was reached. The obtained monolithic block was then crushed, recovered by vacuum filtration, washed with an excess of deionised water and rinsed with acetone. After drying at room temperature, the powder was collected and further purified through Soxhlet extraction for 24 h with acetone. The scheme of the CNN-NS synthesis reaction is shown in figure 1B.

Table 1. Quantities of chemicals used in the synthesis of the three types of CNN-NS

	DMSO		**CNN**		**Et_3N**		**PMDA**		**PMDA/CNN**
	(mL)	(mmol)	(g)	(mmol)	(mL)	(mmol)	(g)	(mmol)	**molar ratio**
CNN-NS (1:2)	20.0	281.6	4.886	7.534	5.0	35.9	3.286	15.067	2
CNN-NS (1:4)	20.0	281.6	4.886	7.534	5.0	35.9	6.573	30.134	4
CNN-NS (1:6)	20.0	281.6	4.886	7.534	5.0	35.9	9.859	45.202	6

153 *2.3 Swelling degree evaluation*

154 Dry CNN-NS specimens of known weights were immersed in buffer solutions with different pH
155 values at room temperature (i.e. pH 2.0, pH 4.0, pH 6.0 and pH 7.4 disodium hydrogen
156 phosphate/phosphoric acid buffer). At pre-determined time intervals, the swollen nanosponges were
157 removed from the buffer, blotted with filter paper to absorb the excess surface solution and
158 immediately weighed. The procedure was repeated until there was no further weight increase. The
159 swelling degree (SD) was then calculated as follows:

$$SD = \frac{(W_t - W_d)}{W_d}$$

160 where W_t is the weight of the swollen nanosponges and W_d is the weight of the nanosponges in the
161 dry state. All experiments were performed in triplicate.

162

163 *2.4 X-ray powder diffraction (XRPD) analysis*

164 To characterise the nanosponges, we carried out a detailed XRPD analysis using a Siemens D5000
165 diffractometer (Cu Kα1, Bragg-Brentano geometry, sequential collection between 2.5° and 60° 2θ).
166 The diffraction patterns were analysed using Fityk software (Wojdyr, 2010).

167

168 *2.5 DSC analysis*

169 Differential Scanning Calorimetry (DSC) was carried out by means of a Perkin Elmer DSC/7
170 differential scanning calorimeter (Perkin-Elmer, CT-USA) equipped with a TAC 7 /DX instrument
171 controller. The instrument was calibrated with indium for melting point and heat of fusion. A
172 heating rate of 10°C/min was employed in the 25-250°C temperature range. Standard aluminium
173 sample pans (Perkin-Elmer) were used; an empty pan was used as a reference standard. Analyses
174 were performed in triplicate on 3 mg samples under nitrogen purge.

175

176 *2.6 Preparation of doxorubicin-loaded CNN-nanosponges (1:4)*

177 An aqueous suspension of the CNN-NS(1:4) at the concentration of 10 mg/ml was prepared. A pre-
178 homogenisation was carried out for 10 min of Ultraturrax (Ika, Germany) at 24,000 rpm. The
179 aqueous suspension was then transferred into a high pressure homogeniser (HPH) (Emulsiflex C5,
180 Avestin, USA) and subjected to homogenisation. The protocol tuned consists of 5 cycles at 5,000
181 psi for 5 min, 12 cycles at 7,000 for 90 min. The obtained aqueous nanosuspension was purified by
182 dialysis and stored at 4°C. An aqueous solution of doxorubicine (2 mg/ml) was incubated at room
183 temperature with the CNN nanosuspension under mild stirring for 12 hours. Subsequently, a

dialysis step was performed to eliminate the unloaded doxorubicin. For cell experiments the nanosuspension was prepared in NaCl 0.9% w/v aqueous solution.

2.7 Quantitative determination of doxorubicin

The quantitative determination of doxorubicin was carried out by a HPLC system consisting of a pump (LC-9A PUMP C, Shimadzu, Japan) equipped with a fluorescence detector (Chrompack, Japan). Analyses were performed using an Agilent TC C_{18} column (250 mm × 4.6 mm, 5 μm). The mobile phase was a mixture of 0.01 M KH_2PO_4 (pH 1.4), acetonitrile and methanol (65:25:10 v/v/v), degassed and pumped through the column at a flow rate of 1 ml/min. The column effluent was monitored at excitation and emission wavelengths of 480 and 560 nm, respectively. The external standard method was used to calculate the drug concentration. For this purpose, 1 mg of doxorubicin was weighed, placed in a volumetric flask, and dissolved in water to obtain a stock standard solution. This solution was then diluted using the mobile phase, providing a series of calibration solutions, subsequently injected into the HPLC system. The linear calibration curve was obtained over the concentration range of 0.025−2.5 μg/ml with a regression coefficient of 0.999.

2.8 Determination of doxorubicin encapsulation efficiency

A 10 mg/mL aqueous suspension of the freeze-dried loaded nanosponges was prepared using filtered water and doxorubicin extracted by sonication for 5 minutes at room temperature. After centrifugation, the drug concentration in the supernatant was determined by the HPLC method previously described. Encapsulation efficiency and drug loading were then calculated using the calibration curve.

2.9 Size, polydispersity index and zeta potential values

CNN-NS sizes and polydispersity indices were measured by dynamic light scattering using a 90 Plus particle sizer (Brookhaven Instruments Corporation, USA) equipped with MAS OPTION particle sizing software. The measurements were made at a fixed angle of 90° for all samples, which were suitably diluted with filtered and distilled water for every measurement. The zeta potential measurements were also taken using an additional electrode in the same instrument. For zeta potential determination, samples of the three formulations were diluted with 0.1 mM KCl and placed in the electrophoretic cell, where an electric field of about 15 V/cm was applied.

2.10 Solid state NMR analysis

Solid state NMR spectra were acquired using a Jeol ECZR 600 instrument, operating at 600.17 and 150.91 MHz for 1H and 13C nuclei, respectively. Powder samples were packed into cylindrical zirconia rotors with a 3.2 mm OD and a 60 µL volume. A certain amount of sample was collected from each batch and used without further preparations to fill the rotor. 13C CPMAS spectra were acquired at a spinning rate of 20 kHz using a ramp cross-polarisation pulse sequence with a contact time of 3.5 ms, a 90° 1H pulse of 2.189 µs, (optimised) recycle delays of 3.5 s (doxorubicin), 1.9s (blank CNN-NS (1:4)) and 0.4s (doxorubicin-loaded CNN-NS(1:4)) and a number of scans included between 2000 and 10000, depending on the sample. For every spectrum a two pulse phase modulation (TPPM) decoupling scheme was used, with a radiofrequency field of 108.5 kHz. The chemical shift scale was calibrated through the methylenic signal of external standard glycine (at 43.7 ppm).

2.11 Morphology analysis

Transmission electron microscopy (TEM) was used to evaluate particle shape and morphology. A Philips CM 10 transmission electron microscope was used and the particle size was measured using the NIH image software. The nanosponge suspensions were sprayed on Formwar-coated copper grid and air-dried before observation.

Scanning electron microscopy (SEM) was used to evaluate the morphology of the CNN-NS formulations using a JEOL JSM IT300LV (EHT 20 kV, working distance 10 mm). The nanosponges were positioned on a conductive sample holder and sputtered with graphite to assure the conductivity of the sample.

2.12 ATR FTIR analysis

ATR FTIR analysis was applied to doxorubicin-loaded CNN-NS, free doxorubicin and plain CNN-NS using a Perkin Elmer 2000 instrument. The spectra were recorded between 400 and 4000 cm^{-1}.

2.13 Stability evaluation of CNN-nanosponges

The physical stability of CNN-NS was evaluated over time, determining size, surface charge and doxorubicin loading, as previously described. This thermal stability of CNN-NS can allow for sterilisation by autoclaving for cell experiments.

2.14 In vitro release of doxorubicin from CNN-nanosponges (1:4)

The *in vitro* release was carried out using multi-compartment rotating cells with a dialysis membrane (Sartorius, cut off 12,000 Da). The donor phase consisted of nanosponge formulation containing a fixed amount of doxorubicin in phosphate buffer at pH 7.4 (1 ml). The receiving phase consisted of phosphate buffer, pH 7.4 or pH 5.5 added with 0.5% w/v sodium lauryl sulphate (1 ml) to maintain proper sink conditions. The receiving phase was completely withdrawn and replaced with fresh medium after fixed time intervals, suitably diluted and analysed using the HPLC method described above.

2.15 Biological assays

2.15.1 Haemolytic activity of CNN-nanosponges

CNN-NS (10 mg/mL) were incubated at 37°C for 90 minutes with 1 ml of diluted blood. Freshly prepared PBS (pH 7.4) was used for all dilution purposes. After incubation, blood-containing suspensions were centrifuged at 2,000 rpm for 10 min to separate the plasma. The amount of haemoglobin released due to haemolysis was measured spectrophotometrically at 543 nm (Du 730, Beckman). The haemolytic activity was calculated with reference to blank and complete haemolysed samples (induced by the addition of ammonium sulphate 20% w/v). Optical microscopy was also used to see if there were any abnormalities in the blood cells after incubation. The observations were made with reference to the blank diluted blood. No changes in red blood cell morphology were detected.

2.15.2 In vitro cytotoxicity determination

The ovarian cell line, A2780, was obtained from the American Type Culture Collection (Rockville, MD, USA). The cells were grown as a monolayer culture in RPMI 1640 medium supplemented with 10% heat-inactivated fetal calf serum (FCS), 2 mmol/l L-glutamine and penicillin/streptomycin (100 units/ml), at 37°C in 5% CO_2 humidified atmosphere.

2.15.3 Colony-forming assay

Cells (1,000 per well) were seeded into six-well plates and treated with the compounds. The medium was changed after 72 h and cells were cultured for an additional 10 days without any drug. Subsequently, the cells were fixed and stained with a solution of 80% crystal violet (Sigma-Aldrich) and 20% methanol for 30 min. The cells were then perfectly washed and 30% acetic acid was added

to induce a complete dissolution of the crystal violet. Absorbance was recorded at 595 nm by a 96-well-plate ELISA reader. Five different experiments were performed.

2.15.4 In vitro uptake study

5 x 10^4 cell/well of A2780 cells were seeded in 24-well plates in 1 ml of culture medium and treated with 10^{-7} M free Doxorubicin or CNN Doxorubicin**.** 48 h (T48) later the cells cultured on the coverslips were rinsed three times with cold PBS and fixed with 75% ethanol for 30 min at 4°C and the coverslips were inverted and mounted on glass slides. The nuclei were stained with 4′,6′-diamidino-2-phenylindole (DAPI 1 mg·mL-1; Sigma-Aldrich, Saint Louis, MO, USA). The slides were analysed by confocal laser scanning microscopy (CLSM) using a Leica DMIRE2 confocal fluorescence microscope (Leica Microsystems AG, Wetzlad, Germany) equipped with Leica Confocal Software v. 2.61.

2.16. Statistical analysis

Data are shown as mean ± SEM. Statistical analyses were performed with GraphPad Prism 3.0 software (La Jolla, CA, USA) using one-way ANOVA and Dunnett's test. Values of $P < 0.05$ were considered statistically significant.

3. Results and Discussion

One strategy to improve the therapeutic effectiveness and to reduce the side effects of anticancer drugs on healthy cells is to improve local drug concentrations at the disease tissues. Biocompatible nanoparticles containing drugs can provide a site-specific delivery of anticancer drugs in a controlled and sustained manner improving the safety profile (Brigger, Dubernet & Couvreur, 2002). Nanoscaled delivery systems can carry loaded drugs to the tumour site through the bloodstream, taking advantage of the enhanced permeability and retention (EPR) effect, due to the defective vascular architecture of the tumour (Fang, Nakamura & Maeda, 2011, Maeda, Nakamura & Fang, 2013). Stimuli-responsive polymer nanoparticles can allow more precise and controlled release behaviour (Cheng, Meng, Deng, Klok & Zhong, 2013). Based upon these concepts, a new nanodelivery system has been developed, using a biocompatible tetraglucose, i.e. cyclic nigerosyl-1-6-nigerose (CNN), as an innovative building block. Solid cross-linked polymer nanoparticles, named cyclic nigerosyl-1-6-nigerose based nanosponges (CNN-NS) were prepared, by the reaction of CNN with pyromellitic dianhydride, to obtain pH resposiveness. Figure 1B reports the schematic representation of the CNN-NS synthesis reaction.

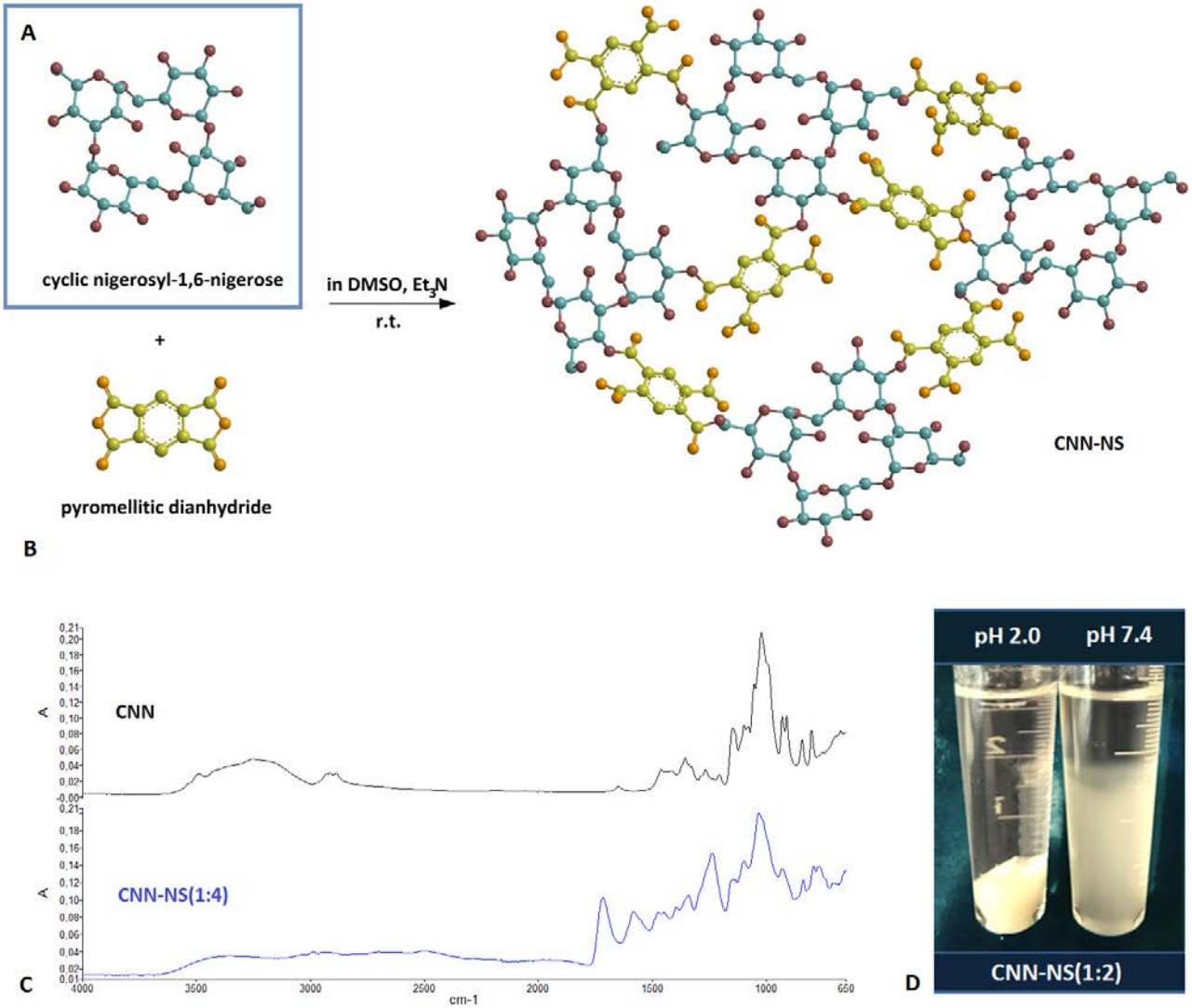

Figure 1. A) Chemical structure of cyclotetraglucose (CNN) **B)** Scheme of the CNN-NS synthesis reaction **C)** ATR-FTIR spectra of CNN and CNN-NS **D)** Swelling capacity of CNN-NS (1:2) as a function of pH values (pH 2 and 7.4).

PMDA was selected, among several cross-linkers, for its high reactivity towards hydroxyl groups, which allows fast reactions with high yields and because of the interactions that carboxylic groups of pyromellitic bridges may establish with polar moieties of drugs (i.e. -COOH, -NH2, -OH groups). These interactions might contribute to high encapsulation efficiency and slow release kinetics. Moreover, the high content of carboxylic groups, introduced by PMDA, confers a pH-sensitive character to CNN-NS, which may be profitably exploited to modulate the release of loaded drugs. The presence of the cross-linked network was confirmed by FTIR analysis. Indeed, the absorption band typical of carboxylate groups appeared in the FTIR-ATR spectrum of CNN-NS at 1580 cm^{-1}, along with other signals deriving from pyromellitic units (i.e. C=O stretching in

carboxylic groups at 1720 cm^{-1} and C-O stretching in ester groups at 1240 cm^{-1}, approximately) was not detected in the spectrum of pristine CNN (figure 1C).

The synthetic process is one-step, cost-effective and its repeatability and scalability have been confirmed. After synthesis, the solid CNN-NS underwent to the HPH step to decrease the nanoparticle dimensions and to produce smaller sizes and more uniform distribution. Indeed, the CNN-NS sizes were reduced reaching sizes lower than 400 nm.

Here, the optimisation and *in vitro* characterisation of this new tetraglucose-based nanodelivery system are reported. Firstly, the effect of the three different CNN cross-linker ratios (i.e. 1:2, 1:4 and 1:6) on the nanostructue and physico-chemical properties was investigated to characterise the three products. All the obtained CNN-NS are amorphous solids, although CNN as such is markedly crystalline. Figure 2 shows the XRPD diagrams of the three types of CNN-NS compared with that of nigerose.

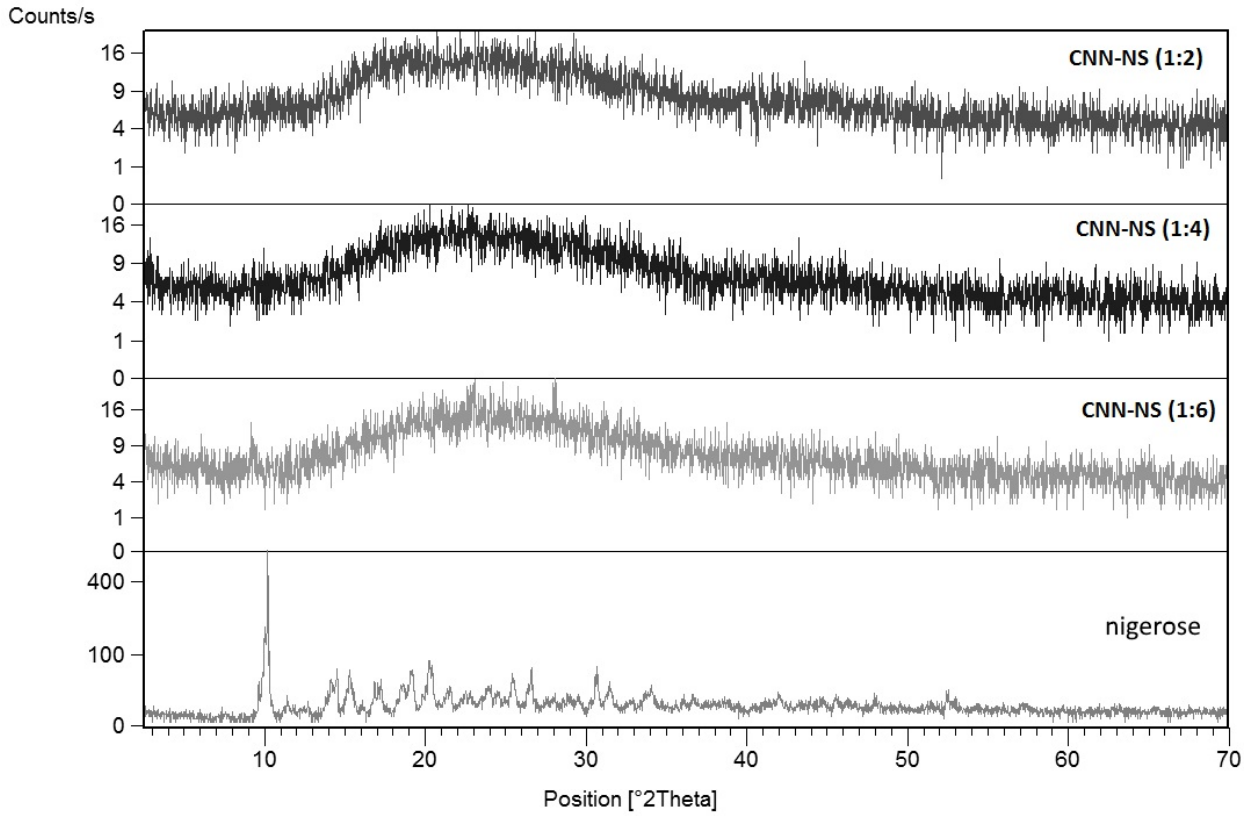

Figure 2. X-ray powder diffraction patterns of the CNN-NS obtained by reacting the CNN with variable concentrations of pyromellityc dianhydride (1:2, 1:4, 1:6 respectively) compared with the XRPD of the nigerose (bottom).

Despite the high degree of crystallinity displayed by nigerose, CNN-NS highlight their amorphous behaviour, shown by the broad bump in the range 10-40 °2θ.

The amorphous nature was confirmed by DSC analyses. No peaks correlated to thermal changes were observed until 250°C (data not shown).

CNN-NS were easily able to absorb water and their swelling capacity was investigated as a function of the pH value of the external environment.

The three types of CNN-NS showed a marked swelling capacity related to the cross-linking degree, which remarkably depends on the pH value (Table 2).

Interestingly, CNN-NS were pH sensitive due to the presence of dissociable carboxylic groups in the polymer matrices. In particular, the swelling degree of the three types of nanosponges linearly increased from pH 2.0 to pH 7.4.

Table 2 reports the swelling degree of the two nanosponges as a function of pH values of the external medium.

Table 2. Swelling degree of CNN-NS as a function of pH values of the external medium.

Sample	**Swelling degree (%)**			
	pH 2.0	**pH 4.0**	**pH 6.0**	**pH 7.4**
CNN-NS (1:2)	562	680	765	820
CNN-NS (1:4)	124	215	307	415
CNN-NS (1:6)	88	206	248	392

It can be seen that CNN-NS (1:2) demonstrated a higher water uptake capability at all the pH values than those of the other two CNN-NS with higher degrees of cross-linking (Figure 1D).

Indeed, the lower the cross-linking degree, the higher the observed swelling. Interestingly, CNN-NS can be considered a quasi super-absorbent material, that was able to retain more than 800 wt% of water at room temperature and pH 7.4.

In this work, doxorubicin was selected as a model drug. Doxorubicin is one of the most common anticancer drug, but it suffers of severe side effects and multidrug resistance. Therefore a nanoformulation to improve its pharmacokinetics and biodistribution would be valuable. Preliminary explorative experiments proved that CNN-NS (1:4) were the most suitable for loading and storing doxorubicin. As a consequence, this type of CNN-NS was selected for further investigation and characterization with the drug.

Table 3 reports the physico-chemical characterization of doxorubicin-loaded and unloaded CNN-NS (1:4).

Table 3. Physico-chemical characterization of blank and doxorubicin-loaded CNN-NS

	CNN-NS (1:4) (unloaded)	**Doxorubicin-loaded CNN-NS (1:4)**
Average diameter ± SD (nm)	355.6 ± 27.3	360.8 ± 15.6
PDI	0.20 ± 0.02	0.19 ± 0.03
PZ ± SD (mV)	- 30.2 ± 4.55	- 29.2 ± 5.29
Loading capacity (%)	-	15.5
Encapsulation efficiency (%)	-	95.1

Doxorubicin encapsulation in CNN-NS did not require high-energy processes or solvent use preserving the drug from potential degradation. Interestingly, it is incorporated by incubation at room temperature under mild stirring. Doxorubicin is a hydrophilic drug with a good aqueous solubility (10 mg/ml). The hydrophilicity of the polymer mesh and probably the polarity of the CNN cavity provide drug encapsulation with high efficiency. The polymer network should play the

key role in the drug incorporation. Indeed, the CNN monomer possesses only a shallow saucer-like shape with a small concave at the center, confirmed by X-ray crystallographic analysis (Bradbrook et al., 2000, Yang et al., 2012). Considering this CNN architecture, the doxorubicin might be mainly entrapped in the hydrophilic nanochannels of the polymer network. The drug loading was 15.5% for doxorubicin-loaded CNN-NS (1:4), with an encapsulation efficiency of about 95%.

Figure 3 shows the SEM (A) and TEM (B) images of CNN-NS before and after HPH step respectively.

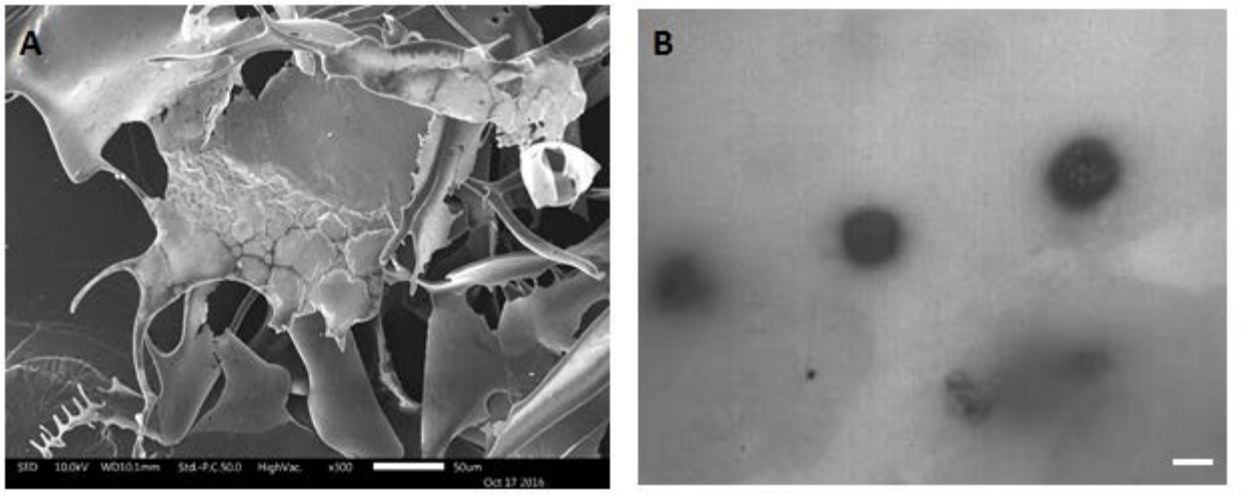

Figure 3. A) SEM image of CNN-NS before HPH step and **B)** TEM image of the CNN-NS after HPH step (TEM scale bar 300 nm).

Figure 3A shows the irregular morphology and large particle size of NS prior to HPH treatment.

As reported in the literature (Trotta, 2011), dextrin-based NS have generally rather compact structures. Also in the case of CNN-NS, BET analysis revealed surface area values below 2 m^2/g (data not shown). Cyclodextrin- and CNN-NS have nanometric and sub-nanometric intrinsic porosity, deriving from the inner cavities of dextrin monomers and from the interstitial volumes among dextrin monomers. Such molecular-level porosity cannot be discerned by means of scanning electron microscopy. TEM image (Fig. 3B) shows the CNN-NS spherical shape and confirms the nanoscaled sizes, reached after the homogenization process.

When loaded with doxorubicin, CNN-NS lose their frankly amorphous behaviour, increasing their low range ordering. Indeed, the new order does not tally with the structure of crystalline doxorubicin, as shown in Figure 4A. The presence of a few broad diffraction peaks in the diffraction pattern of the loaded CNN-NS demonstrates the formation of a brand new, poorly

ordered phase; that ordering is presumably due to the inkling ordering of the doxorubicin inside the nanosponge.

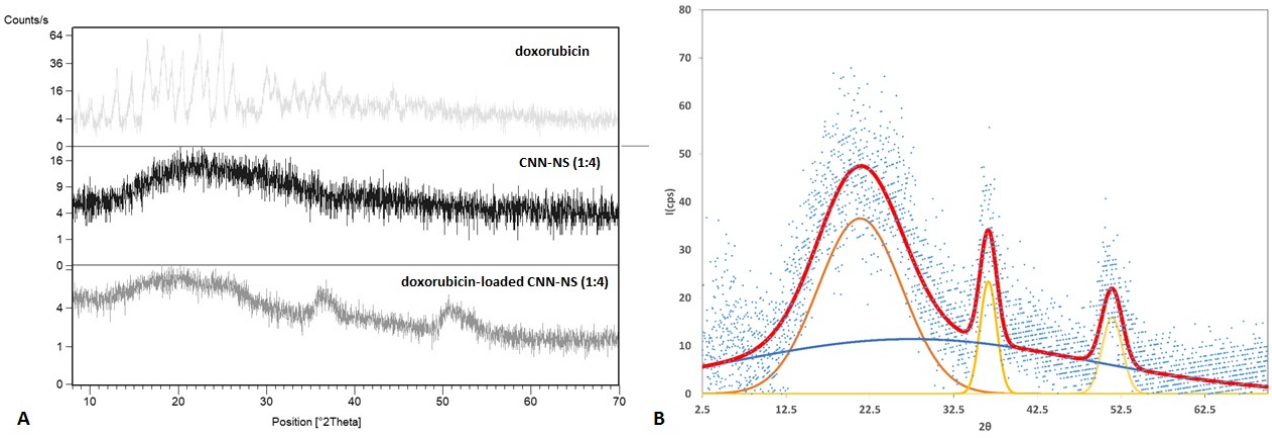

Figure 4. A) CNN-NS (1:4) loading with doxorubicin leads to a deep modification of the nanosponge diffraction pattern (doxorubicin-loaded CNN-NS (1:4) in figure) **B)** Experimental data (dots) and calculated function (red curve) of XRPD of the doxorubicin-loaded CNN-NS. Broad yellow curves represent the decomposition of the XRPD pattern, while the blue one corresponds to the amorphous background.

Table 4: Position, height, area and full width at half maximum of the three diffraction peaks of the CNN 1:4 loaded with doxorubicin

#	Center (°2θ)	Height (cps)	Area (cps)	FWHM (°2θ)
1	21.3426	37.5097	478.982	11.9962
2	36.6454	23.6005	60.563	2.41077
3	51.4022	16.0661	48.7831	2.85251

436 The diffraction data of the CNN 1:4 nanosponges with doxorubicin were decomposed using the
437 Fityk software (Wojdyr, 2010). The decomposition of the XRPD pattern shows at least three curves
438 representing the poor ordering of the system.
439 Due to the broad behaviour of the peaks, a Gaussian profile fitting was selected. The pattern shows
440 a bump (blue line in Figure 4B) ascribable to the amorphous phase and three broad peaks (yellow)
441 possibly related to the weak ordering of the doxorubicin in the loaded nanosponge.
442 DSC analysis of doxorubicin-loaded CNN-NS showed the drug incorporation in the nanosponge
443 matrix (Figure 5A). Indeed, the endothermic peak related to the melting of doxorubicin at about
444 220°C is missing in the thermograms of doxorubicin-loaded CNN-NS, indicating that the drug is
445 molecularly dispersed in the polymer matrix.
446 The cross-linked structure of CNN-NS was confirmed by 13C solid state NMR analysis. Signals
447 deriving from carbonyl groups in ester/carboxylic moieties and aromatic carbon atoms belonging to
448 PMDA units appear at approximately 170 and 130 ppm, respectively (figure 5B).
449 In addition, solid state NMR confirmed the interaction of the drug with CNN-NS.

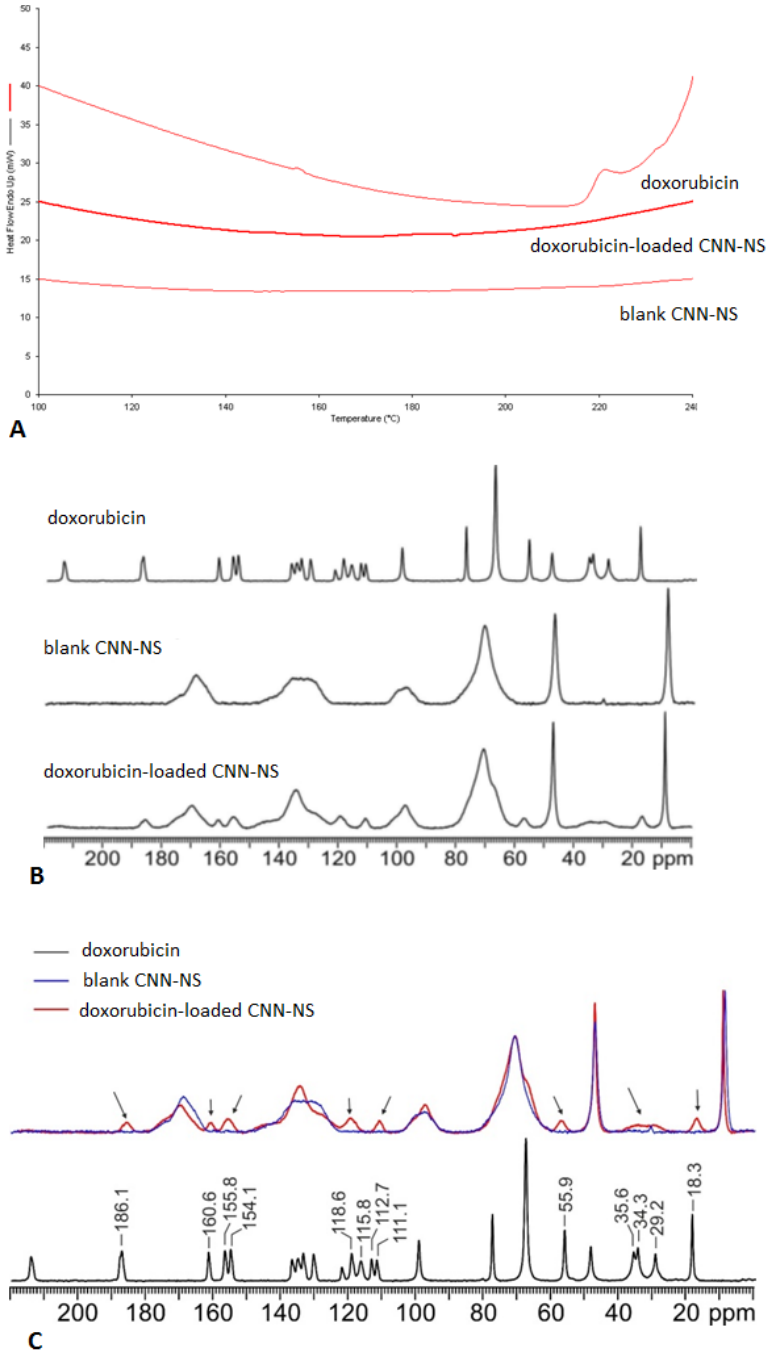

Figure 5. A) DSC thermograms of CNN-NS (1:4), free doxorubicin and doxorubicin-loaded CNN-NS **B)** Solid NMR profiles of CNN-NS (1:4), free doxorubicin and CNN-NS. **C)** Comparison between 13C CPMAS spectra of doxorubicin, blank nanosponge and doxorubicin-loaded CNN-NS in the 0-220 ppm range. Arrows and chemical shift values facilitate the identification of significant peaks.

Figure 5b shows the ^{13}C CPMAS SSNMR spectra of doxorubicin, blank CNN-NS (1:4) and doxorubicin-loaded CNN-NS (1:4). Figure 5c shows the comparison between the spectra of the three samples. In the spectrum of the loaded sample (doxorubicin-loaded CNN-NS, red) several signals, different from the characteristic peaks of the CNN-NS (blank nanosponges, blue), are observed and indicated with arrows. These signals are compliant with the typical chemical shifts of the 13C atoms of doxorubicin (also shown in the figure) and thus evidence the presence of doxorubicin inside the nanosponges.

Then, the *in vitro* doxorubicin release kinetics from CNN-NS was evaluated at pH 5.5 and at pH 7.4 (Figure 6A).

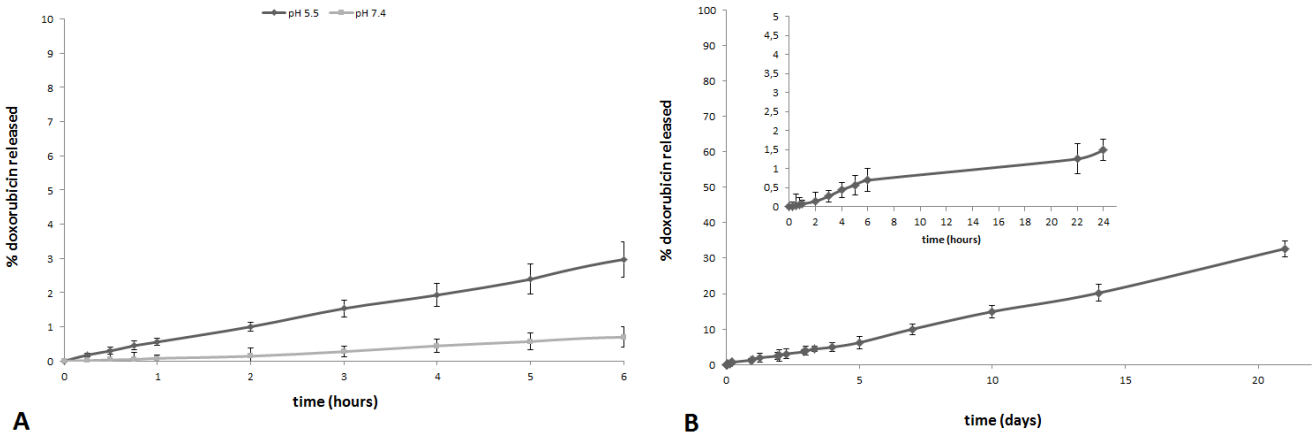

Figure 6. A) *In vitro* release kinetics of doxorubicin from CNN-NS (1:4) as a function of pH; **B)** *In vitro* release kinetics of doxorubicin from CNN-NS (1:4) at pH = 7.4

In vitro release profiles showed a very slow and constant release of the drug over time depending on the pH value of the receiving phase. Interestingly, no burst effect was observed at both pH values. After 24 hours only 1.3% of doxorubicin was released from CNN-NS at pH 7.4, while the percentage of doxorubicin released at pH 5.5 reached 10%. The slow and pH-sensitive release profile may be related to the chemical structure of CNN-NS. The main role is played by the polymer matrix, which comprises free carboxylic groups in the polymer network. The carboxylic groups, belonging from the pyromellitic dianhydride used as cross-linker, are only partially dissociated at pH 5.5 resulting in lower interactions and favouring the drug release. On the other hand, the cavity of CNN monomer is not suitable for doxorubicin complexation being a very small pocket, as previously reported. Considering the β-cyclodextrin-based NS obtained by reacting β-CD

with pyromellitic dianhydride, a doxorubicin release of about 10% was reached after 6 hours at pH 7.4 (data not shown). This different behaviour might be related to the narrow polymer meshes present in CNN-NS. Indeed, the extremely slow and prolonged release behaviour from CNN-NS compared to other doxorubicin nanosponge formulations at pH 7.4 (Cavalli, Trotta & Tumiatti, 2006) might represent an advantage to limit the drug blood exposure and the toxicity of doxorubicin.

We speculate that doxorubicin may be released in a controlled manner following Fickian kinetics due to drug diffusion through the polymeric matrix, which underwent degradation with a very slow kinetics due to hydrolysis. Indeed, the absence of any burst effect could indicate that doxorubicin is not adsorbed on the nanosponge surface and CNN-NS are slowly degraded in the physiological environment.

The release mechanism was further evaluated. The doxorubicin *in vitro* release from drug-loaded CNN-NS was fitted to four distinct models to determine which one exhibited the highest correlation with the experimental results. For each model, the rate constant and correlation values were obtained by applying a linear regression fit. The zero-order kinetic model demonstrated the higher correlation, showing R^2 values of 0.9969 and 0.9985 for doxorubicin release at pH 7.4 and pH 5.5, respectively.

The *in vitro* release kinetics of doxorubicin from CNN-NS at pH 7.4 was followed up to 21 days (Figure 6B).

Intriguingly, the results indicate that at physiological pH value, CNN-NS provide a slow drug diffusion and controlled release over a lengthy period. Indeed, after 14 days at pH 7.4 only about 20% of the drug was released and after 21 days this reached about 32.5%. This behaviour could be exploited to obtain a constant drug concentration in tumour tissue in loco-regional treatment (Cheng et al., 2017, Cinar et al., 2017). Interestingly, the tumour environment pH is more acid than that of normal tissue (Manchun, Dass & Sriamornsak, 2012).

In order to verify the absence of nanosponge activity, cells were treated with plain CNN-NS at dilutions corresponding to that drug-loaded CNN-NS. In all the concentrations tested, the results overlapped with those obtained in controls, with no significant inhibition of cell proliferation, thus excluding any toxic effect of the nanocarriers.

Concerning CNN-NS safety, no significant hemolysis caused by CNN-NS either blank or doxorubicin loaded was observed, confirming their good biocompatibility and the presence of tonicity values suitable for a future potential *in vivo* administration.

Clonogenic survival assays were performed. The cells were seeded 6-well plates and treated with each compound. The culture medium was changed after 72 h, and the cells were cultured for an additional 10 days in the absence of the compounds. The results showed that doxorubicin or CNN doxorubicin treatments differently inhibited the ability of the A2780 cell line to form colonies. In fact, both formulations induced the maximum effect at 10^{-7}M, but doxorubicin-loaded CNN-NS were able to induce a higher inhibition of the colony formation at 10^{-8}-10^{-9}M, determining growth inhibition around 80% and 50%, respectively. Conversely, the treatment with doxorubicin in solution produced a smaller inhibition of the ability to form colonies (50%) at 10^{-8} M, being no more active at the lower concentration.

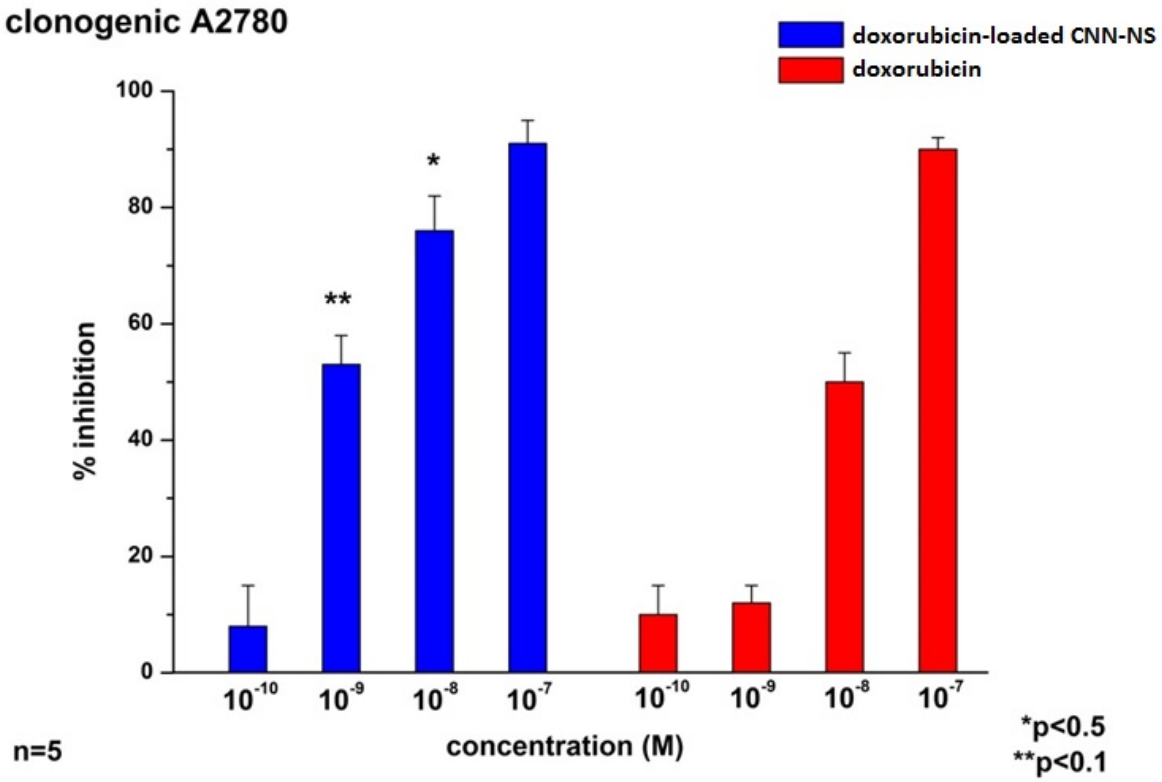

Figure 7. Effect of doxorubicin and doxorubicin-loaded CNN-NS on cell clonogenicity was tested by colony forming assay. A2780 cells (1000 per well) were seeded in six-well plates and treated with each drug at the indicated concentrations for 72 h. The medium was then changed and cells were cultured for additional 10 days and subsequently fixed and stained with crystal violet. Data shown are means ±SEM (n = 5). **P < 0.01, *P < 0.05 significantly different from the same concentration of doxorubicin.

Indeed, the IC_{50} was 0.9±0.2 x 10^{-9}M and 8.5±1 x 10^{-9}M, respectively for doxorubicin-loaded CNN-NS and for free doxorubicin. Therefore, the cytotoxicity of doxorubicin loaded in nanosponges was enhanced of about 8 fold than free drug on A2780 cell lines.

Cell uptake is promoted by nanocarriers as previously shown with various nanoformulations (Miglietta, Cavalli, Bocca, Gabriel & Gasco, 2000, Ernsting, Murakami, Roy, & Li, 2013, Wang et al., 2016). The size, surface charge and the components of CNN-NS might favored the cell internalization. Indeed, *in vitro* uptake results demonstrated that fluorescence was localized in the cytoplasm around the nucleus to a greater extent in the cells treated with doxorubicin-loaded CNN-NS, indicating that CNN-NS had been internalised in a greater extent into the cells.

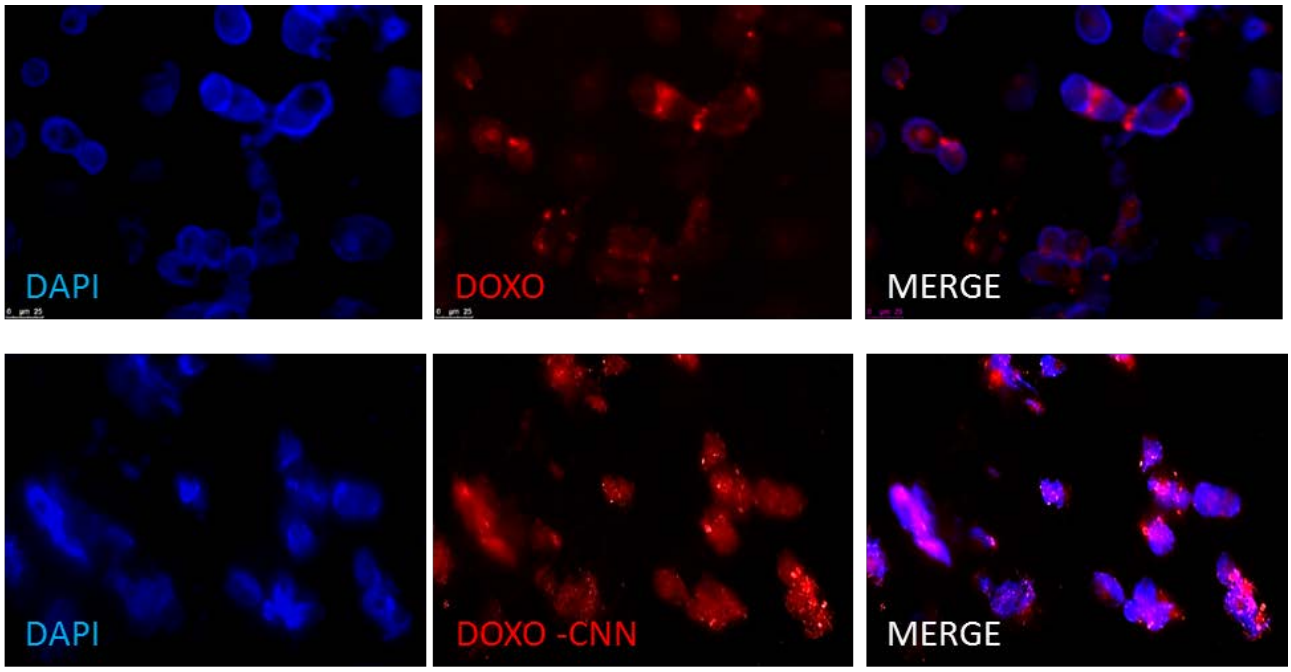

Figure 8. Cell uptake was evaluated by fluorescence microscopy analysis using different doses of doxorubicin-loaded CNN-NS (DOXO-CNN) o free DOX on A2780 cells for 48 h.

Clonogenic assay or colony formation assay is an *in vitro* cell survival assay based on the ability of a single cell to grow into a colony. Only a fraction of seeded cells retains the capacity to produce colonies. After plating at very low density (800 cells for wells), cells are treated with the compounds for 72h, thus they were washed with the cell medium, to remove drugs, and were then allowed to grow over an extended period of time (10 days). Doxorubicin-loaded CNN-NS may act as intracellular drug reservoir slowly releasing the free drug into the cellular cytoplasm, enhancing its therapeutic efficacy. Doxorubicin encapsulation in CNN-NS might increase its concentration at

555 the tumor site, thereby decreasing the frequent dose administered and subsequently reducing the
556 side effects. In this *in vitro* assay, free DOX is also able to inhibit the colony formation, especially
557 at the highest concentration tested (10^{-7}M), considering the static conditions of the experimental set-
558 up. We can hypothesize a different behaviour *in vivo.* Various factors controlled the
559 pharmacokinetics, biodistribution and intratumoral penetration of nanoparticles after their *in vivo*
560 administration (Ernsting et al., 2013). A crucial role is played by the EPR effect, that allows the
561 nanoparticles to escape from the vessels and enter in the tumor cells.
562
563 **4. Conclusions**
564 A new polymer-based nanomaterial was obtained, exploiting a tetraglucose, i.e. CNN, as a
565 monomer in the synthetic reaction. The cross-linking reaction with pyromellitic dianhydride formed
566 solid nanoparticles, named nanosponges. This new nanomaterial is biocompatible and is able to
567 swell in response to the pH value. CNN-NScan be formulated as nanoscale particles with spherical
568 shape suitable for drug delivery. Doxorubicin was incorporated in a good extent and released with a
569 very slow and constant kinetics. Interestingly, the environment pH play a role in controlling the
570 release profile of the drug.
571 Based on the results, doxorubicin-loaded CNN-NS might act as a nanomedicine tool for tumor local
572 treatment with a favorable toxicology profile.
573
574 **Acknowledgements**
575 R. Cavalli and C Dianzani was funded by University of Turin (ex-60 %) funds.
576 The authors thanks prof. Roberto Gobetto and Ms. Federica Rossi for SS-NMR analyses.
577
578 **Author contribution**
579 FC synthetized the CNN-nanosponges, MA and MT formulated and *in vitro* characterized the
580 nanoformulations, LG and CD performed cell culture experiments, LP and DA performed XRPD
581 analyses, FT and RC designed the experiments and gave the intellectual rationale to the work, TN
582 and TH samples gift and chemical information on cyclic nigerosyl-1-6-nigerose.
583

References

- Aga, H., Nishimoto, T., Kuniyoshi, M., Maruta, K., Yamashita, H., Higashiyama, T., Nakada, T., Kubota, M., Fukuda, S., Kurimoto, M., Tsujisaka, Y. (2003). 6-α-Glucosyltransferase and 3-α-Isomaltosyltransferase from Bacillus globisporus N75. *Journal of Bioscience and Bioengineering*, 95(3), 215-224.
- Arpicco, S., Battaglia, L., Brusa, P., Cavalli, R., Chirio, D., Dosio, F., Gallarate, M., Milla, P., Peira, E., Rocco, F., Sapino, S., Stella, B., Ugazio, E., Ceruti, M. (2016). Recent studies on the delivery of hydrophilic drugs in nanoparticulate systems. *Journal of Drug Delivery Science and Technology*, 32, 298-312.
- Bastiancich, C., Scutera, S., Alotto, D., Cambieri, I., Fumagalli, M., Casarin, S., Rossi, S., Trotta, F., Stella, M., Cavalli, R., Musso, T., Castagnoli, C. (2014). Cyclodextrin-Based Nanosponges as a Nanotechnology Strategy for Imiquimod Delivery in Pathological Scarring Prevention and Treatment. *Journal of Nanopharmaceutics and Drug Delivery*, 2(4), 311-324.
- Bhattacharjee, S., Sarkar, B., Sharma, A.R., Gupta, P., Sharma, G., Lee, S.S., Chakraborty, C. (2016). Formulation and Application of Biodegradable Nanoparticles Based Biopharmaceutical Delivery - An Efficient Delivery System. *Curr Pharm Des.* 22(20),3020-3033.
- Bradbrook, GM., Gessler, K., Cote, GL., Momany, F., Biely, P., Bordet, P., Perez, S., Imberty ,A. (2000). X-ray structure determination and modeling of the cyclic tetrasaccharidecyclo-(→6)-α-D-Glc*p*-(1→3)-α-D-Glc*p*-{1→6)-α-D-Glc*p*-(1→3)-α-Glc*p*-(1→}. *Carbohydr Res.*329, 655–665.
- Brigger, I., Dubernet, C., Couvreur, P. (2002). Nanoparticles in cancer therapy and diagnosis. *Advanced Drug Delivery Reviews*, 54(5), 631-651.
- Cavalli, R., Ansari, A.K., Bisazza, A., Giustetto, P., Trotta, F., Vavia, P.R. (2010). Nanosponge formulations as oxygen delivery systems. *Internation Journal of Pharmaceutics*, 402, 254-257.
- Caldera, F., Tannous, M., Cavalli, R., Zanetti, M.,Trotta, F. (2017). Evolution of cyclodextrin nanosponges. International journal of pharmaceutics, 531(2), 470-479.
- Cavalli, R., Trotta, F.,Tumiatti, W. (2006). Cyclodextrin-based nanosponges for drug delivery. *Journal of inclusion phenomena and macrocyclic chemistry*, 56(1-2), 209-213.

- Cheng, R., Meng, F., Deng, C., Klok, H.A., Zhong, Z. (2013). Dual and multi-stimuli responsive polymeric nanoparticles for programmed site-specific drug delivery. *Biomaterials,* 34(14), 3647-3657.
- Cheng, W., Nie, J., Xu, L., Liang, C., Peng, Y., Liu, G., Wang, T., Mei, L., Huang, L., Zeng, X. (2017). pH-Sensitive Delivery Vehicle Based on Folic Acid-Conjugated Polydopamine-Modified mesoporous Silica Nanoparticles for Targeted Cancer Therapy. *ACS Applied Material and Interfaces,* 9(22), 18462-18473.
- Cinar, G., Ozdemir, A., Hamsici, S., Gunay, G., Dana, A., Tekinay A.B., Guler, M.O. (2017). Local delivery of doxorubicin through supramolecular peptide amphiphile nanofiber gels. *Biomaterial Science*, 5, 67–76.
- Daga, M., Ullio, C., Argenziano, M., Dianzani, C., Cavalli, R., Trotta, F., Ferretti, C., Zara, G.P., Gigliotti, C.L., Ciamporcero, E.S., Pettazzoni, P., Corti, D., Pizzimenti, S. (2016). GSH-targeted nanosponges increase doxorubicin-induced toxicity "in vitro" and "in vivo" in cancer cells with high antioxidant defenses. *Free Radical Biology and Medicine*, 97, 24-37.
- Dinarvand, R., Sepehri, N., Manoochehri, S., Rouhani, H., Atyabi F. (2011). Polylactide-co-glycolide nanoparticles for controlled delivery of anticancer agents. *International Journal of Nanomedicine*, 6, 877-95.
- Duchene, D., Cavalli, R., Gref, R. (2016). Cyclodextrin-based polymeric nanoparticles as efficient carriers for anticancer drugs. *Current pharmaceutical biotechnology*, 17(3), 248-255.
- Ernsting, M.J., Murakami, M., Roy, A., & Li, S. D. (2013). Factors controlling the pharmacokinetics, biodistribution and intratumoral penetration of nanoparticles. *Journal of controlled release*, 172(3), 782-794.
- Fang, J., Nakamura, H., Maeda, H. (2011). The EPR effect: Unique features of tumor blood vessels for drug delivery, factors involved, and limitations and augmentation of the effect. *Advanced Drug Delivery Reviews,* 63(3), 136-15.
- Gigliotti, C.L., Ferrara, B., Occhipinti, S., Boggio, E., Barrera, G., Pizzimenti, S., Giovarelli, M., Fantozzi, R., Chiocchetti, A., Argenziano, M., Clemente, N., Trotta, F., Marchiò, C., Annaratone, L., Boldorini, R., Dianzani, U., Cavalli, R., Dianzani C. (2017). Enhanced cytotoxic effect of camptothecin nanosponges in anaplastic thyroid cancer cells in vitro and in vivo on orthotopic xenograft tumors. *Drug Delivery,* 24(1), 670-680.

- Hamidi, M., Azadi, A., Rafiei, P., Ashrafi, H. (2013). A pharmacokinetic overview of nanotechnology-based drug delivery systems: an ADME-oriented approach. *Crit Rev Ther Drug Carrier Syst*. 30(5), 435-67.
- Ishikawa, H., Kuwano, H., Chaen, H., Matsumoto, K. (2009). Complexation of Some Aromatic Compounds with Cyclic Nigerosyl–(1→ 6)–Nigerose. *Journal of Faculty of Agriculture, Kyushu University*, 54(1), 201-204.
- Jaimes-Aguirre, L., Gibbens-Bandala, B.V., Morales-Avila, E., Ocampo-García, B.E., Seyedeh-Fatemeh, M., Amirhosein, A. (2016). Polymer-Based Drug Delivery Systems, Development and Pre-Clinical Status. *Curr Pharm Des.* 22(19), 2886-903.
- Jaimes-Aguirre, L., Morales-Avila, E., Ocampo-García, B.E., Medina, L.A., López-Téllez, G., Gibbens-Bandala, B.V., Izquierdo-Sánchez, V. (2017). Biodegradable poly(D,L-lactide-co-glycolide)/poly(L-γ-glutamic acid) nanoparticles conjugated to folic acid for targeted delivery of doxorubicin. *Materials Science and Engineering C, Materials for Biological Applications*, 76, 743-751.
- Khan, I., Gothwal, A., Sharma, A.K., Kesharwani, P., Gupta, L., Iyer, A.K., Gupta U. (2016). PLGA Nanoparticles and Their Versatile Role in Anticancer Drug Delivery. *Critical Reviews in Therapeutic Drug Carrier Systems*, 33(2), 159-93.
- Lembo, D., Swaminathan, S., Donalisio, M., Civra, A., Pastero, L., Aquilano, D., Vavia, P., Trotta, F. , Cavalli R. (2013). Encapsulation of Acyclovir in new carboxylated cyclodextrin-based nanosponges improves the agent's antiviral efficacy. *International Journal of Pharmaceutics*, 443(1-2), 262-72.
- Liang, W., Yang, C., Zhou, D., Haneoka, H., Nishijima, M., Fukuhara, G., Mori, T., Catiglione F., Mele, A., Caldera, F., Trotta, F., Inoue, Y. (2013). Phase-controlled supramolecular photochirogenesis in cyclodextrin nanosponges. *Chemical Communications*, 49(34), 3510-3512.
- Liang, W., Zhao, M., Wei, X., Yan, Z., Wu, W., Caldera, F., Trotta, F., Inoue, Y., Su, D., Zhong, Z., Yang, C. (2017). Photochirogenic nanosponges: phase-controlled enantiodifferentiating photoisomerization of (Z)-cyclooctene sensitized by pyromellitate-crosslinked linear maltodextrin. *RSC Advances*, 7(28), 17184-17192.
- Liu, X., Yang, Y., Urban, M.W. (2017). Stimuli-Responsive Polymeric Nanoparticles. *Macromol Rapid Commun*. 38(13).

- Maeda, H., Nakamura, H., Fang, J. (2013). The EPR effect for macromolecular drug delivery to solid tumors: Improvement of tumor uptake, lowering of systemic toxicity, and distinct tumor imaging in vivo. *Advanced Drug Delivery Reviews,* 65(1), 71-79.
- Manchun, S., Dass, C.R., Sriamornsak, P. (2012). Targeted therapy for cancer using pH-responsive nanocarrier systems. *Life Sciences,* 90(11-12), 381-387.
- Miglietta, A., Cavalli, R., Bocca, C., Gabriel, L., Gasco, M.R. (2000). Cellular uptake and cytotoxicity of solid lipid nanospheres (SLN) incorporating doxorubicin or paclitaxel. *International Journal of Pharmaceutics,* 210(1), 61-67.
- Muankaew, C., & Loftsson, T. (2018). Cyclodextrins-based Formulations: A Non-Invasive Platform for Targeted Drug Delivery. *Basic & clinical pharmacology & toxicology*, 122, 46-55..
- Mura, S., Nicolas, J., Couvreur, P. (2013). Stimuli-responsive nanocarriers for drug delivery. *Nature materials,* 12(11), 991-1003.
- Natarajan, J.V., Nugraha, C., Ng, X.W., Venkatraman, S. (2014). Sustained-release from nanocarriers: a review. *Journal of Controlled Release,* 193, 122-138.
- Nishimoto, T., Aga, H., Mukai, K., Hashimoto, T., Watanabe, H., Kubota, M., Fukuda, S. Kurimoto, M., Tsujisaka, Y. (2002). Purification and Characterization of Glucosyltransferase and Glucanotransferase Involved in the Production of Cyclic Tetrasaccharide in Bacillus globisporus C11. *Bioscience. Biotechnology. Biochemistry,* 66(9), 1806-1818.
- Oku, K., Kudou, N., Kurose, M., Shibuya, T., Chaen, H., Fukuda, S. (2007). The crystal properties of cyclic nigerosyl-(1-6)-nigerose (CNN) and powdering of alpha-tocopherol, cholecalciferol and EPA using CNN. *Journal of the Japanese Society for Food Science and Technology (Japan).*
- Prasad, M., Lambe, U. P., Brar, B., Shah, I., Manimegalai, J., Ranjan, K., Rao, R. Kumar,S., Mahant, S., Khurana, S.K., Iqbal, H.M., Dhama, K., Misri, J., Prasad, G. (2018). Nanotherapeutics: An insight into healthcare and multi-dimensional applications in medical sector of the modern world. *Biomedicine & Pharmacotherapy,* 97, 1521-1537.
- Sherje, A. P., Dravyakar, B. R., Kadam, D., & Jadhav, M. (2017). Cyclodextrin-based nanosponges: a critical review. *Carbohydrate polymers*, 173, 37-49.
- Swaminathan, S., Cavalli, R., Trotta, F., Ferruti, P., Ranucci, E., Gerges, I., Manfredi, A., Marinotto, D., Vavia P.R. (2010a). In vitro release modulation and conformational

stabilization of a model protein using swellable polyamidoamine nanosponges of β-cyclodextrin. *Journal of Inclusion Phenomena and Macrocyclic Chemistry*, 68(1-2), 183-191.

- Swaminathan, S., Pastero, L., Serpe, L., Trotta, F., Vavia, P., Aquilano, D., Trotta, M., Zara, G.P., Cavalli, R. (2010b). Cyclodextrin-based nanosponges encapsulating camptothecin: physicochemical characterization, stability and cytotoxicity. *European Journal of Pharmaceutics and Biopharmaceutics*, 74, 193-201.
- Torne, S., Ansari, K., Vavia, P.R., Trotta, F., Cavalli, R. (2010). Enhanced oral paclitaxel bioavailability after administration of paclitaxel-loaded nanosponges. *Drug Delivery*, 17(6), 419-425.
- Trotta, F. (2011). Cyclodextrin Nanosponges and Their Applications. *Cyclodextrins in Pharmaceutics, Cosmetics, and Biomedicine*, Wiley, Hoboken.
- Trotta, F., Zanetti, M., Cavalli, R. (2012). Cyclodextrin-based nanosponges as drug carriers. *Beilstein Journal of Organic Chemistry*, 8, 2091-2099.
- Trotta, F., Dianzani, C., Caldera, F., Mognetti, B., Cavalli, R. (2014). The application of nanosponges to cancer drug delivery. *Expert Opinion on Drug Delivery*, 11(6), 931-941.
- Wang, H. X., Zuo, Z. Q., Du, J. Z., Wang, Y. C., Sun, R., Cao, Z. T., Ye, X., Wang, J., Leong, K.W., Wang, J. (2016). Surface charge critically affects tumor penetration and therapeutic efficacy of cancer nanomedicines. *Nano Today*, 11(2), 133-144.
- Watanabe, H., Nakano, M., Oku, K., Aga, H., Nishimoto, T., Kubota, M., Fukuda, S., Kurimoto, M., and Tsujisaka Y. (2004). Cyclic tetrasaccharides in sake lees. *J. Appl. Glycosci*. 51, 345-347
- Wei, X., Liang, W., Wu, W., Yang, C., Trotta, F., Caldera, F., Mele, A., Nishimoto, T., Inoue, Y. (2015). Solvent-and phase-controlled photochirogenesis. Enantiodifferentiating photoisomerization of (Z)-cyclooctene sensitized by cyclic nigerosylnigerose-based nanosponges crosslinked by pyromellitate. *Organic & biomolecular chemistry*, 13(10), 2905-2912.
- Weissenfeld, M. (2005). Hydrolysis determination of CT-11 at different pH values. Unpublished study report of RCC Ltd. for Hayashibara International, Inc., Westminster, USA. 11 March, 2005.
- Wojdyr, M.J. (2010). Fityk: a general-purpose peak fitting program. *Journal of Applied Crystallography*, 4(5), 1126-1128

- Yang, C., Liang, W., Nishijima, M., Fukuhara, G., Mori, T., Hiramatsu, H., ... & Inoue, Y. (2012). Supramolecular Photochirogenesis with Novel Cyclic Tetrasaccharide: Enantiodifferentiating Photoisomerization of (Z)-Cyclooctene with Cyclic Nigerosylnigerose-Based Sensitizers. *Chirality*, 24(11), 921-927